


Multiband Quantum Criticality of Polar Metals

Pavel A. Volkov^{1,2,*} and Premala Chandra^{1,2}¹Department of Physics and Astronomy, Rutgers University, Piscataway, New Jersey 08854, USA²Center for Materials Theory, Rutgers University, Piscataway, New Jersey 08854, USA (Received 26 March 2020; accepted 27 May 2020; published 12 June 2020; corrected 25 August 2020)

Motivated by recent experimental realizations of polar metals with broken inversion symmetry, we explore the emergence of strong correlations driven by criticality when the polar transition temperature is tuned to zero. Overcoming previously discussed challenges, we demonstrate a robust mechanism for coupling between the critical mode and electrons in multiband metals. We identify and characterize several novel interacting phases, including non-Fermi liquids, when band crossings are close to the Fermi level and present their experimental signatures for three generic types of band crossings.

DOI: 10.1103/PhysRevLett.124.237601

Metals close to quantum critical points (QCPs) are strongly correlated systems that often exhibit non-Fermi liquid behavior [1] and novel orderings including unconventional superconductivity [2]. Studies of metals near spin density wave [3,4], ferromagnetic [5] and nematic QCPs [6] indicate that the behaviors of quantum critical metals depend crucially on the nature of the QCPs involved. Recent discoveries [7–13] and predictions [14–16] of a number of polar metals [17] that undergo an inversion symmetry breaking transition, structurally similar to a ferroelectric one [18] (whose QCP properties are also actively studied [19–24]) suggest a novel avenue of metallic quantum criticality to be explored.

Here we perform a systematic study of quantum critical polar metals and possible strong correlations therein. We show the critical polar mode to be strongly coupled to *interband* particle-hole excitations (Fig. 1). Since unconventional metallic quantum criticality occurs when critical bosons are coupled to gapless excitations, we study quantum critical polar metals with Fermi energies pinned to electronic band crossings; we present evidence of strong renormalization of the polar phonon spectra and non-Fermi liquid behavior of the charge carriers (Fig. 1).

Experimentally, intrinsic [8,25,26] and engineered [7,9,12,27,28] polar metals exist; the former include several layered transition metal dichalcogenides [10,13,29] with more predicted [14–16]. Furthermore the search for Weyl semimetals has led to more polar (semi-)metals [30]. Chemical tuning of polar transition temperatures has been demonstrated [9,31–33]. Here we make predictions for experimental signatures of the novel phases that we identify in quantum critical polar metals.

An important challenge for the realization of correlated polar metals is that the critical boson (a polar optical phonon [34]) of a polar metallic QCP does not couple easily to the electronic degrees of freedom; proposed couplings that involve order parameter gradients [35–39]

and/or nonlinearities [40] are usually irrelevant in the scaling sense at a QCP [1]. Additionally, Coulomb interactions play a special role here, leading to a splitting between longitudinal and transverse modes when the screening is weak [34,41,42], although this effect may be smaller for certain ferroelectric systems [43,44].

Here we show that a Yukawa coupling of the order parameter (φ) to carriers, $H_Y = \lambda \int d\mathbf{r} \varphi(\mathbf{r}) c^\dagger(\mathbf{r}) c(\mathbf{r})$, known to induce strong correlations for other types of QCPs [3–6], can be generically realized in multiband systems even without spin-orbit coupling (SOC) (that has been previously considered [45–48]), leading to the most pronounced interaction effects at band crossings. Using symmetry-based classification of such crossings, we analyze possible strongly coupled metallic behaviors near polar QCPs, including long-range Coulomb effects.

Yukawa coupling to the polar critical mode.— We look for fermionic bilinears $\hat{O}^i(\mathbf{k})$ such that $\varphi^i \int d\mathbf{k} \hat{O}^i(\mathbf{k})$

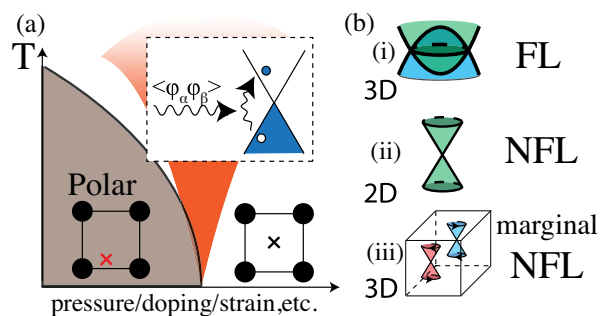


FIG. 1. (a) Schematic phase diagram of a polar metal with a critical region around the QCP. Inset illustrates that the critical fluctuations couple to an interband excitation. (b) Summary of the QCP behaviors near typical band crossing: (i) a 3D nodal line, (ii) a 2D nodal point, and (iii) 3D Weyl points. (N)FL stands for (Non-)Fermi liquid; in all cases the polar mode is strongly renormalized. Coulomb interactions introduce anisotropy for (i) and (ii), and gap the longitudinal mode for (iii).

respects inversion symmetry, first assuming time-reversal symmetry \mathcal{T} . Since the order parameter breaks inversion symmetry, $\mathcal{P}^{-1}\varphi^i\mathcal{P} = -\varphi^i$, we thus seek a fermionic bilinear $\hat{O}^i(\mathbf{k})$ that breaks inversion but not time-reversal symmetry.

For a single conduction band without SOC, the only possible form of $\hat{O}(\mathbf{k})$ is $\hat{c}_{\mathbf{k}}^\dagger f_0(\mathbf{k}) \hat{c}_{\mathbf{k}}$. Since both \mathcal{P} and \mathcal{T} require f_0 to be even, it is not possible for $\hat{O}(\mathbf{k})$ to break only inversion symmetry. However with SOC present, bilinears of the form $\hat{c}_{\mathbf{k}}^\dagger f_i(\mathbf{k}) s_i \hat{c}_{\mathbf{k}}$, where s_i are the Pauli matrices in spin space, are allowed: an odd in \mathbf{k} choice for $f_i(\mathbf{k})$ results in a bilinear that is odd under \mathcal{P} only. We thus conclude that SOC is necessary for a Yukawa polar coupling in a single-band model.

By contrast, in a multiband system a Yukawa coupling can exist without SOC. In a two-band model ignoring spin, \mathcal{T} is complex conjugation and \mathcal{P} acts in band space: $\mathcal{P} \sim \sigma_0$ for bands with the same parity or $\mathcal{P} \sim \sigma_3$ (up to a unitary transformation) in the opposite case. Writing a generic fermionic bilinear as $\hat{c}_{\mathbf{k}}^\dagger [f_0(\mathbf{k}) + \sum_{i=1}^3 f_i(\mathbf{k}) \sigma_i] \hat{c}_{\mathbf{k}}$, we find that the terms breaking inversion, but not time reversal, symmetries are even in \mathbf{k} $f_i(\mathbf{k})$ for $\mathcal{P} \sim \sigma_3$ or odd in \mathbf{k} $f_2(\mathbf{k})$ for $\mathcal{P} \sim \sigma_0$. We can thus have the following Yukawa couplings to the polar mode at $\mathbf{q} \approx 0$

$$\begin{aligned} H_{\text{coupl}}^{(a)} &= \sum_{i,\mathbf{q},\mathbf{k}} f_a^i(\mathbf{k}) \varphi_{\mathbf{q}}^i c_{\mathbf{k}+\mathbf{q}/2}^\dagger \sigma_1 c_{\mathbf{k}-\mathbf{q}/2}, & \mathcal{P} \sim \sigma_3 \\ H_{\text{coupl}}^{(b)} &= \sum_{i,\mathbf{q},\mathbf{k}} f_b^i(\mathbf{k}) \varphi_{\mathbf{q}}^i c_{\mathbf{k}+\mathbf{q}/2}^\dagger \sigma_2 c_{\mathbf{k}-\mathbf{q}/2}, & \mathcal{P} \sim \sigma_0, \end{aligned} \quad (1)$$

where $f_{a(b)}^i(\mathbf{k})$ is even(odd) in \mathbf{k} , and the order parameter couples to an *interband* bilinear [Fig. 1(a), inset].

If we assume the bands originate from two distinct orbitals, the physical mechanism of this Yukawa polar coupling can be illustrated (Fig. 2). If the orbitals have different parity (e.g., s and p) [Fig. 2(a)], they are mixed linearly by an inversion-breaking perturbation (similar to the Stark effect). This mixing is reflected in a nonzero

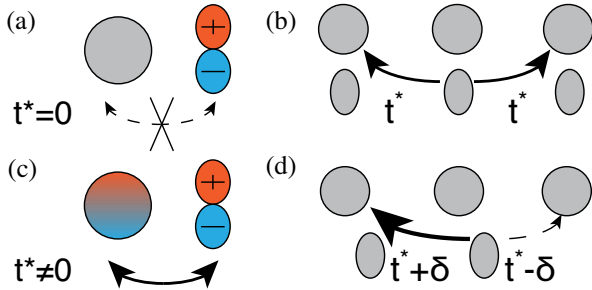


FIG. 2. Illustration of the coupling to the polar order parameter for two orbitals having (a),(c) opposite and (b),(d) same parity under inversion. (a) and (b) The symmetric phase $\varphi^i = 0$, (c) and (d) the state for $\varphi^i \neq 0$. In both cases, interorbital hopping changes, as reflected in Eq. (1).

constant hybridization between the resulting bands, forbidden in the symmetric phase [Fig. 2(a)]. Because of the necessity of \mathbf{k} dependence, the same-parity case [Fig. 2(b)] cannot be viewed as local. We exemplify it by a nearest-neighbor hopping between the orbitals [Fig. 2(b)]; absence of inversion symmetry yields distinct left and right interorbital hoppings from a given site, similar to the dimerization occurring in the SSH model [49]. Similar effects have been considered in studies of SrTiO₃ interfaces [50,51].

Band crossings and low-energy theory.—To drive unconventional metallic behavior already at weak coupling, the interband particle-hole excitations coupled to the critical mode with Eq. (1) need to be gapless. This is possible close to momenta where the two bands cross; a low-energy theory can then be constructed around these band crossings if they occur close to the Fermi energy. This situation can be realized due to filling considerations (as, e.g., in graphene) or by carrier doping. Here we study the polar QCP when the Fermi energy is at the band crossing. Neglecting SOC, \mathcal{PT} symmetry to protected line crossings in 3D systems [52–54] and point nodes in two dimensions [54]. For completeness, we also study a polar QCP in a \mathcal{T} -breaking driven Weyl semimetal [55–57].

Having identified the three generic types of band crossings, we next turn to their emergent metallic behaviors at the polar QCPs. We study the limit $T = 0^+$ at the QCP itself, analyzing each case both with and without long-range Coulomb interactions. The latter situation is relevant when (i) inversion symmetry breaking in the insulating system does not produce a macroscopic dipole moment (e.g., when the transition is to a structure with a nonpolar point group that does not allow for a macroscopic dipole moment [58] or in the case of elemental materials) or if (ii) there exist additional Fermi pockets that lead to strong screening. In the absence of (ii), screening of the Coulomb interaction will depend on the type of the band crossing.

3D nodal lines.—We consider a minimal Hamiltonian with a circular nodal line in the k_x, k_y plane,

$$\begin{aligned} H_{\text{line}} &= \sum_{\mathbf{k}} c_{\mathbf{k}}^\dagger \left[\frac{k_x^2 + k_y^2 - k_F^2}{2m} \sigma_3 + \gamma k_z \sigma_2 \right] c_{\mathbf{k}}, \\ H_{\text{coupl}} &= \lambda \sum_{\mathbf{q},\mathbf{k}} \varphi_{\mathbf{q}} c_{\mathbf{k}+\mathbf{q}/2}^\dagger \sigma_1 c_{\mathbf{k}-\mathbf{q}/2}, \end{aligned} \quad (2)$$

which corresponds to taking $f_i = \text{const}$ in Eq. (1) (as is discussed below, this does not affect the qualitative results). Only a single order parameter component can couple to fermions near a single nodal line. In principle, isotropy is restored when two additional nodal lines that couple to the other order parameter components are present—e.g., three $p_{x,y,z}$ -like bands crossing an s -like one; then there are three nodal lines, each coupled to the corresponding component of the order parameter $\varphi_{x,y,z}$. However, as we will show now, it is sufficient to consider Eq. (2) with straightforward generalizations.

We begin by considering the lowest-order bosonic self-energy, following the Hertz approach [59]. Our calculations [60] yield

$$\Pi(i\omega, \mathbf{q}) - \Pi(0, 0) = -\frac{\lambda^2 m \rho(\omega, q_r, q_z)}{4\pi\gamma} E\left(\frac{(v_F q_r)^2}{\rho(\omega, q_r, q_z)^2}\right), \quad (3)$$

where $\rho(\omega, q_r, q_z) = \sqrt{\omega^2 + (v_F q_r)^2 + (\gamma q_z)^2}$ and $E(x)$ is an elliptic integral of the second kind. Gapless fermions lead to the damping of the critical mode: $\Pi(i\omega, \mathbf{q}) \sim |\omega|$ at low \mathbf{q} ($v_F q, \gamma q \ll \omega$) similar to the situation at spin-density wave QCPs [3]. However, unlike that case, Eq. (3) is strongly momentum dependent, leading to an unchanged dynamical critical exponent, i.e., $z = 1$. Once the bosonic self-energy is taken into account, a scaling analysis with the scheme of Ref. [66] yields the scaling dimensions of Yukawa and quartic interboson couplings to be $(2-d)/2$ and $1-d$, respectively, making both irrelevant in the $d = 3$ nodal line case. An explicit calculation [60] of the fermionic self-energy and vertex corrections with a screened bosonic propagator also indicates the absence of infrared divergences, showing that the scaling limit of Eq. (2) is captured by Hertz-Millis theory. We note, however, that a recent RG analysis using a different momentum shell scheme [67] suggests nontrivial corrections to the Hertz-Millis fixed point away from the large- N_f limit (N_f being the number of fermionic flavors; for additional discussion see Ref. [60]).

We now address the role of a momentum-dependent fermion-boson coupling within Hertz-Millis theory: since at the QCP the only relevant term is the bosonic self-energy, a momentum-dependent coupling would just result in replacing λ^2 in Eq. (3) with its Fermi surface average. Next we address the role of Coulomb interaction. Assuming that the Fermi liquid state is robust at the QCP, we know from previous work [66,68] that screening by nodal line electrons results in a renormalized Coulomb interaction $\propto q^{-1}$, while further effects of the Coulomb interaction are irrelevant in the RG sense and can be considered perturbatively. The coupling between renormalized Coulomb interaction and the polar phonon affects the critical propagator

$$D_{\text{Coul}}^{-1}(i\omega, \mathbf{q}) = -\Pi(i\omega, \mathbf{q}) + V_{\text{Coul}}^{NL}(\mathbf{q}) Q_0^2 q^2 \cos^2 \eta,$$

where η is the angle between \mathbf{q} and the polarization direction of φ and Q_0 —the effective charge of the polar mode. Since $V_{\text{Coul}}^{NL}(\mathbf{q}) \sim q^{-1}$ [66,68], the Coulomb interaction does not change the scaling properties of the critical mode but rather introduces an anisotropy.

2D Dirac point.—We consider a Hamiltonian $H_{\text{point}} = \sum_{\mathbf{k}} c_{\mathbf{k}}^\dagger v_F (k_x \sigma_x + k_y \sigma_y) c_{\mathbf{k}}$ and coupling $H_{\text{coupl}} = \lambda \sum_{\mathbf{q}, \mathbf{k}} \varphi_{\mathbf{q}} c_{\mathbf{k}+\mathbf{q}/2}^\dagger \sigma_3 c_{\mathbf{k}-\mathbf{q}/2}$ (we take $\mathcal{P} \sim \sigma_1$ here). Again we

find the order parameter to be scalar, similar to what occurs at a CDW transition in graphene [69,70], which breaks the inversion (but not translational) symmetry and is associated with charge imbalance between two sublattices.

In the absence of Coulomb interactions, this model is equivalent to the Gross-Neveu-Yukawa (GNY) model [71,72] whose critical properties have been studied extensively [73,74]. Its critical point is known to have emergent Lorentz invariance and $z = 1$; it follows then that the critical phonon velocity (c_s) is renormalized such that $c_s/v_F \rightarrow 1$. The anomalous dimensions for both the bosons and the fermions further demonstrates the non-Fermi liquid behavior at the QCP.

We now include Coulomb interactions, first considering their effect on the critical boson, whose propagator is now

$$D(i\omega, \mathbf{q}) = \frac{1}{(\omega^2 + c^2 q^2) + 2\pi Q_0^2 q_x^2 / q}, \quad (4)$$

while the Coulomb interaction takes the form

$$V_{\text{Coul}}(i\omega, \mathbf{q}) = \frac{2\pi(\omega^2 + c^2 q^2)}{q(\omega^2 + c^2 q^2) + 2\pi Q_0^2 q_x^2}. \quad (5)$$

This renormalization changes the bare scaling dimension of q_x : $[q_x] = [\omega, q_y]^{3/2}$. Consequently, the renormalized Coulomb interaction becomes irrelevant for the fermions ($[e] = -1/4$), while the Yukawa coupling remains relevant ($[\lambda] = 1/4$). In order to determine the critical properties at this fixed point we perform one-loop momentum-shell RG calculations in two dimensions; details are provided in Ref. [60], where we introduce an additional parameter, the number of nodal points N_f . We note that the fermionic and bosonic renormalizations are determined by different dimensionless couplings, $\beta_\varphi = (\lambda^2 Z_\varphi^2 a_\varphi) / (2\pi^2 v_{Fy}^3 Z_\psi \Lambda)$ and $\beta_\psi = (\lambda^2 Z_\varphi) / (2\pi^2 v_{Fy}^2 \sqrt{2\pi Q_0^2 \Lambda})$, respectively, where $Z_{\psi, \varphi}$ are the quasiparticle residues and $\Lambda = \Lambda_0 e^{-l}$ is the running RG scale. We find the resulting solution of the RG equations to exhibit a runaway flow for $\beta_\varphi \sim e^{2l/5}$, while $\beta_\psi \sim 2/l$ goes to zero. Most importantly, we find that the Fermi velocities along the two directions are renormalized differently: $dv_{Fy}/dl < 0$; $dv_{Fx}/dl > 0$, with v_{Fy} eventually flowing to zero as $e^{l/5}$ [60]. Enhanced anisotropy is also present in the bosonic behavior, with $c_x^2 \sim e^l$; $c_y^2 \sim \text{const}$. Taking $l \sim \log[k^{-1}, \omega^{-1}]$, we use the asymptotic solutions to obtain the following forms of critical propagators (where $\alpha, \beta, \delta, \gamma, \rho$ are constants):

$$D(i\omega, \mathbf{q}) \sim \frac{1}{\alpha\omega + c_y^2 q_y^2 + 2\pi Q_0^2 q_x^2 / q + \beta q_x},$$

$$G(i\varepsilon, \mathbf{k}) \sim \frac{1}{\delta i\varepsilon^{0.8} + \gamma \sigma_x k_x^{0.8} + \rho \sigma_y k_y^{1.2}}. \quad (6)$$

Weyl points in 3D QC polar metals.—Neglecting possible anisotropies, we find the Weyl Hamiltonian and the Yukawa coupling to take the form

$$\begin{aligned}
 H_W &= \sum_{\mathbf{k}} c_{\mathbf{k}}^\dagger v_F (\vec{k} \cdot \vec{\sigma}) c_{\mathbf{k}}, \\
 H_{\text{coupl}} &= \lambda \sum_{\mathbf{q}, \mathbf{k}} \vec{\varphi}_{\mathbf{q}} c_{\mathbf{k}+\mathbf{q}/2}^\dagger \vec{\sigma} c_{\mathbf{k}-\mathbf{q}/2}.
 \end{aligned} \quad (7)$$

Since the interaction is marginal, we use the perturbative RG to probe the system's behavior. Importantly, the bosonic self-energy evaluated on the momentum shell is

$$\delta\Pi_{\alpha\beta} = -\frac{\lambda^2}{\pi^2 v_F^3} \frac{\omega^2 + v_F^2 (q^2 \delta_{\alpha\beta} - q_\alpha q_\beta)}{12} dl \quad (8)$$

and we see that the longitudinal mode is unrenormalized while the transverse one hardens. The full RG equations are presented in the Supplemental Material [60]; the RG flows to weak coupling with the large- l asymptotic $\alpha \rightarrow 2/(N_f l \log l)$, where $\alpha \equiv (\lambda^2 Z_\varphi^2)/(12\pi^2 Z_\psi v_F^3)$ and N_f is the number of Weyl points in the system (cf. we neglect interpoint coupling since it requires finite momentum transfer). We find $c_L/c_T \rightarrow 0$ due to the hardening of the transverse phonon velocity. The quasiparticle residues for bosons and fermions both vanish ($Z_\psi \propto \text{const}/l$; $Z_\varphi \sim \text{const}/\log l$) which, in conjunction with $l = \log(k^{-1}, \omega^{-1})$, suggests logarithmic non-Fermi liquid corrections. However the bosonic quasiparticle residue vanishes only as $1/\log l$, so the bosons receive only log-log corrections and are relatively well defined at the QCP.

The Coulomb interaction screened by the polar phonon becomes itself irrelevant, but results in the renormalized propagator for the longitudinal mode acquiring a gap. The RG equations are then obtained by disregarding the longitudinal mode's contribution to the fermionic self-energy and vertex renormalization. We note that the longitudinal mode nonetheless receives corrections due to Yukawa coupling; this reflects itself in the behavior of the dielectric constant (see below). The solutions of the RG equations [60] are qualitatively similar to those without Coulomb interactions.

Finally we note that for a 3D Dirac point [75] (that requires additional symmetries to be realized), the RG equations are found to flow to strong coupling, and the critical mode to soften. Since a 3D Dirac point can be thought of as a stable merger of two Weyl points, we attribute this result to inter-Weyl cone scattering that we have not considered due to finite momentum separation between cones Q_w . We thus expect that in the polar phase, where the Dirac point splits into two Weyl ones, the flow to strong coupling will be cut off at a scale set by $v_F Q_w$.

Experimental signatures.—We next discuss simple experimental signatures of the quantum critical polar metallic phases we have identified. The QC (bosonic) specific heat C_{bos} can be estimated with Hertz-Millis theory [60,76] leading to $C_{\text{bos}} \sim T^{d/z}$. In the cases we study, we observe that $z = 1$ except for the nodal point cases with

TABLE I. Summary of Hertz-Millis estimates for the temperature dependencies of resistivity $\rho(T)$ and the bosonic contribution to the specific heat $C_{\text{bos}}(T)$ close to a Polar QCP; here NL and NP are nodal lines and points, respectively, ρ_0 is a constant and $\Delta = 0.5$ when Coulomb interactions are included and 0 otherwise.

Band crossing type	$\lim_{T \rightarrow 0^+} \rho(T)$	$\lim_{T \rightarrow 0^+} C_{\text{bos}}(T)$
3D NL	T^3	T^3
3D NP	T^{-1}	T^3
2D NP	ρ_0	$T^{2-\Delta}$

Coulomb interactions: in two dimensions one momenta scales as $\sqrt{\omega}$ at the QCP which suggests, using Eq. (6), that $C_{\text{bos}} \sim T^{1.5}$; in three dimensions a logarithmic correction is present. We also obtain T -dependent resistivity estimates with a scattering rate calculation using a RPA-screened bosonic propagator [60,77]. These estimates are summarized in Table I.

In all three cases we have studied, the critical polar mode is strongly affected by interactions close to the QCP. For the nodal points the characteristic boson velocity renormalizes to a value of order v_F , suggesting stiffening of the transverse mode. A more complete picture can be given for the Hertz-Millis theory of the nodal line case using Eq. (3) continued to real frequencies. For $q_r = 0$, the transverse has an unusual dispersion $\omega^2 = (cq_z)^2 + \omega_\lambda [\sqrt{4(\gamma^2 - c^2)q_z^2 + \omega_\lambda^2} - \omega_\lambda]/2$ while for the $q_z = 0$ case one has

$$\omega \approx \begin{cases} -i\omega_\lambda & (q \ll \omega_\lambda/v_F), \\ \sqrt{2\omega_\lambda v q/\pi - \frac{i\omega_\lambda^2}{\pi}} & [\omega_\lambda/v_F \ll q \ll (v_F/c)^2 \omega_\lambda/v_F] \\ cq & [(v_F/c)^2 \omega_\lambda/v_F \ll q], \end{cases} \quad (9)$$

where $\omega_\lambda = \lambda^2 m/8\gamma$. Observation of such dispersion renormalization and smearing of the spectral weight may be accessible by inelastic neutron scattering measurements.

Additionally, for the case of 3D nodal semimetals, the bulk ω - and \mathbf{q} -dependent contribution of the polar mode to the dielectric constant $\epsilon(\mathbf{q}, \omega)$ may be obtained from optical conductivity [57] or EELS experiments [78]:

$$\begin{aligned}
 \lim_{v_F q, \gamma q \ll \omega} \epsilon_{NL}^{\text{Pol}}(\mathbf{q}, \omega) &= \frac{4i\pi Q_0^2 \cos^2 \eta}{\omega_\lambda \omega}, \\
 \lim_{q \rightarrow 0} \epsilon_{WP}^{\text{Pol}}(\mathbf{q}, \omega) &= -\frac{4\pi Q_0^2}{\omega^2 (\log \omega^{-1})^{N_f/\kappa_0(N_f)}}, \quad (10)
 \end{aligned}$$

where $N_f/\kappa_0(N_f)$ depends on the number N_f of Weyl points but is of order 1 [60]. We also note that the presence

of a Yukawa-coupled band crossing actually *promotes* polar ordering, since the static part $\Pi(0,0)$ of the bosonic self-energy is positive. This effect is maximal when the Fermi level is at the band crossing and diminishes as it moves away. Of particular interest is the case when symmetries allow nodal surfaces; here the relevant bosonic self-energies would be logarithmically divergent [79] leading to possible realizations of an electronically driven polar order that was proposed some time ago [80] already at weak coupling.

Conclusion.—In this Letter we have shown that nodal multiband metals provide promising platforms for strongly correlated metallic behaviors near polar QCPs. We have demonstrated a generic mechanism for Yukawa-like coupling to the critical mode without spin-orbit coupling. Identifying band crossings to be most affected by the polar QCP, we have studied critical behavior for three distinct cases (2D Dirac and 3D Weyl points, and 3D nodal lines) with and without Coulomb interactions. In our study we find the critical polar mode to be strongly renormalized for all band crossing types, and we have demonstrated the emergence of non-Fermi liquid behavior for the two nodal point cases. Finally we have analyzed thermodynamic, transport, and dielectric properties and the critical mode dispersion for the quantum critical polar metallic phases we have identified. In view of the recent discovery of a number of polar metals with a multiband electronic structure such as LiOsO_3 [8,11], MoTe_2 [10], and WTe_2 [13] and predictions of many more [14–16,33], we hope that our study will provide guidance for the search of exotic metallicity in future experiments on polar metals.

We thank P. Coleman for detailed discussions, particularly in the early development of this project. We are grateful to P. W. Anderson, E. Christou, S. Fang, G. Jose, D. Khomskii, E. König, Y. Komijani, D. Maslov, and B. Uchoa for their helpful comments. P. A. V. acknowledges a Postdoctoral Fellowship from the Rutgers University Center for Materials Theory, and this work was also supported by Grant No. DE-SC0020353 (P. C.) funded by the U.S. Department of Energy, Office of Science.

*pv184@physics.rutgers.edu

- [1] S. Sachdev, *Quantum Phase Transitions* (Cambridge University Press, Cambridge, UK, 1999).
- [2] D. J. Scalapino, A common thread: The pairing interaction for unconventional superconductors, *Rev. Mod. Phys.* **84**, 1383 (2012).
- [3] Ar. Abanov, A. V. Chubukov, and J. Schmalian, Quantum-critical theory of the spin-fermion model and its application to cuprates: Normal state analysis, *Adv. Phys.* **52**, 119 (2003).
- [4] H. Löhneysen, A. Rosch, M. Vojta, and P. Wölfle, Fermi-liquid instabilities at magnetic quantum phase transitions, *Rev. Mod. Phys.* **79**, 1015 (2007).
- [5] M. Brando, D. Belitz, F. M. Grosche, and T. R. Kirkpatrick, Metallic quantum ferromagnets, *Rev. Mod. Phys.* **88**, 025006 (2016).
- [6] T. Shibauchi, A. Carrington, and Y. Matsuda, A quantum critical point lying beneath the superconducting dome in iron pnictides, *Annu. Rev. Condens. Matter Phys.* **5**, 113 (2014).
- [7] T. Kolodiaznyi, M. Tachibana, H. Kawaji, J. Hwang, and E. Takayama-Muromachi, Persistence of Ferroelectricity in BaTiO_3 through the Insulator-Metal Transition, *Phys. Rev. Lett.* **104**, 147602 (2010).
- [8] Y. Shi, Y. Guo, X. Wang, A. J. Princep, D. Khalyavin, P. Manuel, Y. Michiue, A. Sato, K. Tsuda, S. Yu, M. Arai, Y. Shirako, M. Akaogi, N. Wang, K. Yamaura, and A. T. Boothroyd, A ferroelectric-like structural transition in a metal, *Nat. Mater.* **12**, 1024 (2013).
- [9] C. W. Rischau, X. Lin, C. P. Grams, D. Finck, S. Harms, J. Engelmayer, T. Lorenz, Y. Gallais, B. Fauque, J. Hemberger, and K. Behnia, A ferroelectric quantum phase transition inside the superconducting dome of $\text{Sr}_{1-x}\text{Ca}_x\text{TiO}_{3-\delta}$, *Nat. Phys.* **13**, 643 (2017).
- [10] J. Jiang, Z. K. Liu, Y. Sun, H. F. Yang, C. R. Rajamathi, Y. P. Qi, L. X. Yang, C. Chen, H. Peng, C. C. Hwang *et al.*, Signature of type-II Weyl semimetal phase in MoTe_2 , *Nat. Commun.* **8**, 13973 (2017).
- [11] W. Chi Yu, X. Zhou, F.-C. Chuang, S. A. Yang, H. Lin, and A. Bansil, Nonsymmorphic cubic dirac point and crossed nodal rings across the ferroelectric phase transition in LiOsO_3 , *Phys. Rev. Mater.* **2**, 051201 (2018).
- [12] Y. Cao, Z. Wang, S. Y. Park, Y. Yuan, X. Liu, S. M. Nikitin, H. Akamatsu, M. Kareev, S. Middey, D. Meyers, P. Thompson, P. J. Ryan, P. Shafer, A. N'Diaye, E. Arenholz, V. Gopalan, Y. Zhu, K. M. Rabe, and J. Chakhalian, Artificial two-dimensional polar metal at room temperature, *Nat. Commun.* **9**, 1547 (2018).
- [13] Z. Fei, W. Zhao, T. A. Palomaki, B. Sun, M. K. Miller, Z. Zhao, J. Yan, X. Xu, and D. H. Cobden, Ferroelectric switching of a two-dimensional metal, *Nature (London)* **560**, 336 (2018).
- [14] S. N. Shirodkar and U. V. Waghmare, Emergence of Ferroelectricity at a Metal-Semiconductor Transition in a 1T Monolayer of MoS_2 , *Phys. Rev. Lett.* **112**, 157601 (2014).
- [15] R. Fei, W. Kang, and L. Yang, Ferroelectricity and Phase Transitions in Monolayer Group-IV Monochalcogenides, *Phys. Rev. Lett.* **117**, 097601 (2016).
- [16] W. Ding, J. Zhu, Z. Wang, Y. Gao, D. Xiao, Y. Gu, Z. Zhang, and W. Zhu, Prediction of intrinsic two-dimensional ferroelectrics in In_2Se_3 and other $\text{III}_2\text{-VI}_3$ van der Waals materials, *Nat. Commun.* **8**, 14956 (2017).
- [17] N. A. Benedek and T. Birol, “Ferroelectric” metals reexamined: Fundamental mechanisms and design considerations for new materials, *J. Mater. Chem. C* **4**, 4000 (2016).
- [18] P. W. Anderson and E. I. Blount, Symmetry Considerations on Martensitic Transformations: “Ferroelectric” Metals?, *Phys. Rev. Lett.* **14**, 217 (1965).
- [19] D. E. Khmel'nitskii and V. L. Shneerson, Phase-transition of displacement type in crystals at very low temperatures, *Zh. Eksp. Teor. Fiz.* **64**, 316 (1973) [*Sov. Phys. JETP* **37**, 164 (1973)].

- [20] R. Rousev and A. J. Millis, Theory of the quantum paraelectric-ferroelectric transition, *Phys. Rev. B* **67**, 014105 (2003).
- [21] S. E. Rowley, L. J. Spalek, R. P. Smith, M. P. M. Dean, M. Itoh, J. F. Scott, G. G. Lonzarich, and S. S. Saxena, Ferroelectric quantum criticality, *Nat. Phys.* **10**, 367 (2014).
- [22] P. Chandra, G. G. Lonzarich, S. E. Rowley, and J. F. Scott, Prospects and applications near ferroelectric quantum phase transitions: A key issues review, *Rep. Prog. Phys.* **80**, 112502 (2017).
- [23] P. Chandra, P. Coleman, M. A. Continentino, and G. G. Lonzarich, Quantum annealed criticality, [arXiv: 1805.11771](https://arxiv.org/abs/1805.11771).
- [24] A. Narayan, A. Cano, A. V. Balatsky, and N. A. Spaldin, Multiferroic quantum criticality, *Nat. Mater.* **18**, 223 (2019).
- [25] Y. Yoshida, S.-I. Ikeda, H. Matsuhata, N. Shirakawa, C. H. Lee, and S. Katano, Crystal and magnetic structure of $\text{Ca}_3\text{Ru}_2\text{O}_7$, *Phys. Rev. B* **72**, 054412 (2005).
- [26] S. Lei, M. Gu, D. Puggioni, G. Stone, J. Peng, J. Ge, Y. Wang, B. Wang, Y. Yuan, K. Wang, Z. Mao, J. M. Rondinelli, and V. Gopalan, Observation of quasi-two-dimensional polar domains and ferroelastic switching in a metal, $\text{Ca}_3\text{Ru}_2\text{O}_7$, *Nano Lett.* **18**, 3088 (2018).
- [27] T. H. Kim, Danilo Puggioni, Y. Yuan, L. Xie, H. Zhou, N. Campbell, P. J. Ryan, Y. Choi, J.-W. Kim, J. R. Patzner *et al.*, Polar metals by geometric design, *Nature (London)* **533**, 68 (2016).
- [28] P. Nukala, M. Ren, R. Agarwal, J. Berger, G. Liu, A. T. Charlie Johnson, and R. Agarwal, Inverting polar domains via electrical pulsing in metallic germanium telluride, *Nat. Commun.* **8**, 15033 (2017).
- [29] P. Sharma, F.-X. Xiang, D.-F. Shao, D. Zhang, E. Y. Tsymlal, A. R. Hamilton, and J. Seidel, A room-temperature ferroelectric semimetal, *Sci. Adv.* **5**, eaax5080 (2019).
- [30] M. Zahid Hasan, S.-Y. Xu, I. Belopolski, and S.-M. Huang, Discovery of Weyl fermion semimetals and topological fermi arc states, *Annu. Rev. Condens. Matter Phys.* **8**, 289 (2017).
- [31] H. Sakai, K. Ikeura, M. Saeed Bahramy, N. Ogawa, D. Hashizume, J. Fujioka, Y. Tokura, and S. Ishiwata, Critical enhancement of thermopower in a chemically tuned polar semimetal MoTe_2 , *Sci. Adv.* **2**, e1601378 (2016).
- [32] S. Barraza-Lopez, T. P. Kaloni, S. P. Poudel, and P. Kumar, Tuning the ferroelectric-to-paraelectric transition temperature and dipole orientation of group-IV monochalcogenide monolayers, *Phys. Rev. B* **97**, 024110 (2018).
- [33] A. Narayan, Effect of strain and doping on the polar metal phase in LiOsO_3 , *J. Phys. Condens. Matter* **32**, 125501 (2020).
- [34] W. Cochran, Crystal stability and the theory of ferroelectricity, *Adv. Phys.* **9**, 387 (1960).
- [35] L. P. Gor'kov, Phonon mechanism in the most dilute superconductor n-type SrTiO_3 , *Proc. Natl. Acad. Sci. U.S.A.* **113**, 4646 (2016).
- [36] J. Ruhman and P. A. Lee, Superconductivity at very low density: The case of strontium titanate, *Phys. Rev. B* **94**, 224515 (2016).
- [37] P. Wölfle and A. V. Balatsky, Superconductivity at low density near a ferroelectric quantum critical point: Doped SrTiO_3 , *Phys. Rev. B* **98**, 104505 (2018).
- [38] J. Ruhman and P. A. Lee, Comment on “Superconductivity at low density near a ferroelectric quantum critical point: Doped SrTiO_3 ,”, *Phys. Rev. B* **100**, 226501 (2019).
- [39] P. Wölfle and A. V. Balatsky, Reply to “Comment on ‘Superconductivity at low density near a ferroelectric quantum critical point: Doped SrTiO_3 ,’”, *Phys. Rev. B* **100**, 226502 (2019).
- [40] D. van der Marel, F. Barantani, and C. W. Rischau, Possible mechanism for superconductivity in doped SrTiO_3 , *Phys. Rev. Research* **1**, 013003 (2019).
- [41] A. Mooradian and G. B. Wright, Observation of the Interaction of Plasmons with Longitudinal Optical Phonons in GaAs, *Phys. Rev. Lett.* **16**, 999 (1966).
- [42] A. I. Larkin and D. E. Khmel'nitskiĭ, Phase transition in uniaxial ferroelectrics, *Zh. Eksp. Teor. Fiz.* **56**, 2087 (1969) [*Sov. Phys. JETP* **29**, 1123 (1969)].
- [43] K. F. Garrity, K. M. Rabe, and D. Vanderbilt, Hyperferroelectrics: Proper Ferroelectrics with Persistent Polarization, *Phys. Rev. Lett.* **112**, 127601 (2014).
- [44] A. K. Tagantsev, Weak ferroelectrics, *Ferroelectrics* **79**, 57 (1988).
- [45] V. Kozii and L. Fu, Odd-parity Superconductivity in the Vicinity of Inversion Symmetry Breaking in Spin-Orbit-Coupled Systems, *Phys. Rev. Lett.* **115**, 207002 (2015).
- [46] F. Wu and I. Martin, Nematic and chiral superconductivity induced by odd-parity fluctuations, *Phys. Rev. B* **96**, 144504 (2017).
- [47] S. Kanasugi and Y. Yanase, Spin-orbit-coupled ferroelectric superconductivity, *Phys. Rev. B* **98**, 024521 (2018).
- [48] S. Kanasugi and Y. Yanase, Multiorbital ferroelectric superconductivity in doped SrTiO_3 , *Phys. Rev. B* **100**, 094504 (2019).
- [49] W. P. Su, J. R. Schrieffer, and A. J. Heeger, Solitons in Polyacetylene, *Phys. Rev. Lett.* **42**, 1698 (1979).
- [50] A. Joshua, S. Pecker, J. Ruhman, E. Altman, and S. Ilani, A universal critical density underlying the physics of electrons at the $\text{LaAlO}_3/\text{SrTiO}_3$ interface, *Nat. Commun.* **3**, 1129 (2012).
- [51] M. Diez, A. M. R. V. L. Monteiro, G. Mattoni, E. Cobanera, T. Hyart, E. Mulazimoglu, N. Bovenzi, C. W. J. Beenakker, and A. D. Caviglia, Giant Negative Magnetoresistance Driven by Spin-Orbit Coupling at the $\text{LaAlO}_3/\text{SrTiO}_3$ Interface, *Phys. Rev. Lett.* **115**, 016803 (2015).
- [52] Y. Kim, B. J. Wieder, C. L. Kane, and A. M. Rappe, Dirac Line Nodes in Inversion-Symmetric Crystals, *Phys. Rev. Lett.* **115**, 036806 (2015).
- [53] C. Fang, Y. Chen, H.-Y. Kee, and L. Fu, Topological nodal line semimetals with and without spin-orbital coupling, *Phys. Rev. B* **92**, 081201(R) (2015).
- [54] T. Bzdušek and M. Sigrist, Robust doubly charged nodal lines and nodal surfaces in centrosymmetric systems, *Phys. Rev. B* **96**, 155105 (2017).
- [55] A. A. Burkov and L. Balents, Weyl Semimetal in a Topological Insulator Multilayer, *Phys. Rev. Lett.* **107**, 127205 (2011).

- [56] G. B. Halász and L. Balents, Time-reversal invariant realization of the Weyl semimetal phase, *Phys. Rev. B* **85**, 035103 (2012).
- [57] N. P. Armitage, E. J. Mele, and A. Vishwanath, Weyl and dirac semimetals in three-dimensional solids, *Rev. Mod. Phys.* **90**, 015001 (2018).
- [58] H. Klapper and Th. Hahn, Point-group symmetry and physical properties of crystals, in *International Tables for Crystallography* (Wiley, Hoboken, NJ, USA, 2006), Chap. 10.2, pp. 804–808.
- [59] J. A. Hertz, Quantum critical phenomena, *Phys. Rev. B* **14**, 1165 (1976).
- [60] See Supplemental Material at <http://link.aps.org/supplemental/10.1103/PhysRevLett.124.237601> for the details of calculations, which includes Refs. [61–65].
- [61] A. L. Fitzpatrick, S. Kachru, J. Kaplan, and S. Raghu, Non-fermi-liquid fixed point in a Wilsonian theory of quantum critical metals, *Phys. Rev. B* **88**, 125116 (2013).
- [62] M. A. Metlitski and S. Sachdev, Quantum phase transitions of metals in two spatial dimensions. i. Ising-nematic order, *Phys. Rev. B* **82**, 075127 (2010).
- [63] N. Goldenfeld, *Lectures on Phase Transitions and the Renormalization Group* (CRC Press, Boca Raton, 1992), <https://doi.org/10.1201/9780429493492>.
- [64] A. Thakur, K. Sadhukhan, and A. Agarwal, Dynamic current-current susceptibility in three-dimensional Dirac and Weyl semimetals, *Phys. Rev. B* **97**, 035403 (2018).
- [65] J. Zhou and H.-R. Chang, Dynamical correlation functions and the related physical effects in three-dimensional Weyl/Dirac semimetals, *Phys. Rev. B* **97**, 075202 (2018).
- [66] Y. Huh, E.-G. Moon, and Y. Baek Kim, Long-range coulomb interaction in nodal-ring semimetals, *Phys. Rev. B* **93**, 035138 (2016).
- [67] G. Jose and B. Uchoa, Quantum critical scaling of gapped phases in nodal-line semimetals, *Phys. Rev. B* **101**, 115123 (2020).
- [68] J.-W. Rhim and Y. Baek Kim, Anisotropic density fluctuations, plasmons, and Friedel oscillations in nodal line semimetal, *New J. Phys.* **18**, 043010 (2016).
- [69] J. Alicea and M. P. A. Fisher, Graphene integer quantum hall effect in the ferromagnetic and paramagnetic regimes, *Phys. Rev. B* **74**, 075422 (2006).
- [70] J.-N. Fuchs and P. Lederer, Spontaneous Parity Breaking of Graphene in the Quantum Hall Regime, *Phys. Rev. Lett.* **98**, 016803 (2007).
- [71] D. J. Gross and A. Neveu, Dynamical symmetry breaking in asymptotically free field theories, *Phys. Rev. D* **10**, 3235 (1974).
- [72] J. Zinn-Justin, Four-fermion interaction near four dimensions, *Nucl. Phys.* **B367**, 105 (1991).
- [73] L. N. Mihaila, N. Zerf, B. Ihrig, I. F. Herbut, and M. M. Scherer, Gross-neveu-yukawa model at three loops and ising critical behavior of dirac systems, *Phys. Rev. B* **96**, 165133 (2017).
- [74] T. C. Lang and A. M. Läuchli, Quantum Monte Carlo Simulation of the Chiral Heisenberg Gross-Neveu-Yukawa Phase Transition with a Single Dirac Cone, *Phys. Rev. Lett.* **123**, 137602 (2019).
- [75] V. Kozii, Z. Bi, and J. Ruhman, Superconductivity Near a Ferroelectric Quantum Critical Point in Ultralow-Density Dirac Materials, *Phys. Rev. X* **9**, 031046 (2019).
- [76] P. Coleman, C. Pépin, Q. Si, and R. Ramazashvili, How do fermi liquids get heavy and die?, *J. Phys. Condens. Matter* **13**, R723 (2001).
- [77] A. J. Schofield, Non-fermi liquids, *Contemp. Phys.* **40**, 95 (1999).
- [78] S. Vig, A. Kogar, M. Mitrano, A. A. Husain, V. Mishra, M. S. Rak, L. Venema, P. D. Johnson, G. D. Gu, E. Fradkin, M. R. Norman, and P. Abbamonte, Measurement of the dynamic charge response of materials using low-energy, momentum-resolved electron energy-loss spectroscopy (M-EELS), *SciPost Phys.* **3**, 026 (2017).
- [79] P. A. Volkov and S. Moroz, Coulomb-induced instabilities of nodal surfaces, *Phys. Rev. B* **98**, 241107(R) (2018).
- [80] I. B. Bersuker, On the origin of ferroelectricity in perovskite-type crystals, *Phys. Lett.* **20**, 589 (1966).

Correction: The omission of a support statement in the Acknowledgments has been fixed.